

# Real time GPS Positioning of LEO Satellites Mitigating Pseudorange Multipath through Neural Networks

P. RAMOS-BOSCH, M. HERNÁNDEZ-PAJARES, J.M. JUAN and J. SANZ  
Technical University of Catalonia (UPC), Barcelona, Spain

*Received April 2007; Revised October 2007*

**ABSTRACT:** *A method for real-time positioning of LEO satellites using dual frequency GPS receivers is presented. It is based on an a priori ground estimation of a pseudorange multipath map computed by means of a Self-Organizing Map neural network algorithm. The generated map characterizes the multipath environment of the satellite. This a priori estimation allows a real time correction of the pseudorange observables onboard the LEO satellite with a number of parameters affordable for space applications in terms of CPU and memory usage. The novelty of the approach consists of the use of neural networks to reduce the number of parameters and the use of a hybrid offline-online method. Precise IGS clocks and orbits have been used to measure the impact of these corrections in the navigation solution. Improvements in 3D positioning error of about 40%–50% for SAC-C (obtaining errors  $\sim 90\text{cm}$ ) and 25%–35% for CHAMP (obtaining errors  $\sim 70\text{cm}$ ) are demonstrated.*

## INTRODUCTION

Nowadays more and more low Earth orbiting (LEO) satellites are equipped with GPS receivers, and their accurate positioning is becoming an important aspect to the scientific community. Normally, this is done in postprocessing, where present techniques make use of GPS carrier phase measurements, attaining position accuracies of 5 cm with dual-frequency receivers and 10 cm with single-frequency receivers [1]. Nevertheless, some applications, such as Autonomous Formation Flying (AFF) [2] and Space Rendezvous and Docking (RVD) [3], require real time solutions. In this kind of processing, which obviously has to be done on the LEO satellite, the utilization of phase measurements is a more complex task, since it involves the on the fly estimation of the carrier phase ambiguities. In order to avoid carrier phase ambiguity resolution in real time processing, the alternative is to use the code pseudorange measurements, which are unambiguous measurements but have higher multipath and thermal noise errors.

On the other hand, as it is well known, the main source of error in GPS positioning comes from the ionospheric delay. About 99.9% of this error can be removed using the ionospheric-free combination [4] (from now on  $P_C$  for pseudorange measures and  $L_C$

for carrier phase measures) for dual-frequency receivers (several LEO satellites are equipped with this equipment, such as SAC-C, CHAMP, JASON and GPSMET), but this approach increases the pseudorange multipath and thermal noise (among other unmodeled sources of error) by a factor of about three. Multipath is mainly caused by the physical distribution of the satellite body, which leads to a high spatial correlation of close rays (in terms of their incoming directions) so, as it also occurs in fixed ground receivers, the multipath is repeatable with the geometry of rays as seen in Figure 1 for the LEO SAC-C, where three different GPS satellites follow close footprints on the antenna sky plot at different times. The multipath follows the same pattern for all three arcs. The scope of the following method is to mitigate the multipath by taking advantage of this repeatability in order to achieve a better performance when the  $P_C$  combination is used. This is done in two phases: 1) an *a priori* estimation of a multipath map (which characterizes the multipath for each azimuth/elevation direction) that can be computed on the ground with the data of the past few days of the LEO satellite, and 2) an onboard real time multipath correction. In this work, the multipath corrections have been applied to a kinematic LMS single point positioning in order to test the impact of these corrections in the final navigation solution. Positioning using a dynamic orbit model would largely increase the computing needs of the filter,

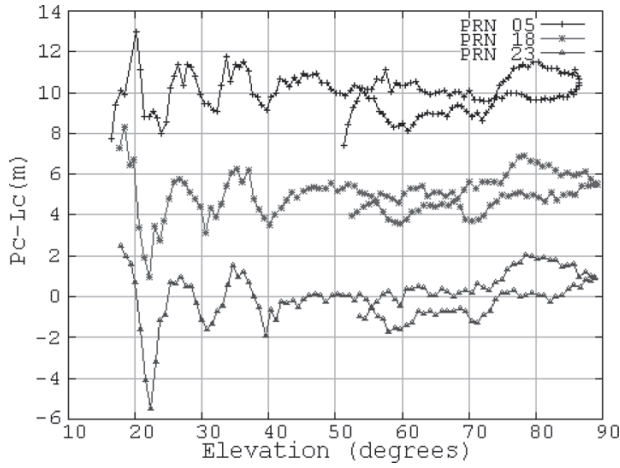


Fig. 1—Repeatability of multipath for different arcs and times. Y axis represents the multipath in meters plus an unknown bias (difference between ionospheric-free pseudorange and carrier phase combinations). Data processed from SAC-C satellite for day 155 of 2002.

and would probably need a simplification of the most common models to do this kind of processing in real time. This is out of the scope of the present work, which aimed to present a low cost method for LEO positioning. Therefore kinematic positioning has been chosen instead, due to its very low requirements in terms of CPU and memory usage.

The idea of characterizing multipath by its incoming directions can be seen in [5], and some efforts have obtained satellite maps, such as [6] for CRISTA-SPAS and [7] for CHAMP. The multipath map would also absorb other direction-dependent effects, such as phase center variations. An example of this could be seen for satellite JASON-1, which has large pseudorange phase center variations depending on the incoming direction (up to 90 cm, as can be seen in [8]). In the presented method, the map is obtained using a Self-Organizing Map algorithm (a type of neural network without classical counterpart, see [9] for more details) in order to minimize the parameters needed to characterize the satellite multipath environment (obtaining the same performance with about half of the parameters).

This method is mainly based on the work done in [10] and has evolved to the present state.

## METHOD

The *a priori* multipath map estimation will provide the multipath detected for a set of given directions which will be called *cell centers*. The multipath for each observation can be obtained by means of a classic observable combination that allows isolating the multipath [5].

In this work, the main observable used is the ionospheric-free pseudorange combination, which is defined as

$$P_c = \frac{f_1^2 P_1 - f_2^2 P_2}{f_1^2 - f_2^2} = \rho + c(dt_{rec} - dt^{sat}) + rel + M_{P_c} + \varepsilon_{P_c} \quad (1)$$

where  $f_1$  and  $f_2$  are the frequencies of the GPS signals (1575.42 MHz and 1227.60 MHz, respectively),  $P_1$  and  $P_2$  are the pseudorange codes for both frequencies,  $\rho$  is the geometric range between the receiver at the time of reception and the GPS satellite at the time of transmission,  $c$  is the speed of light,  $dt_{rec}$  is the difference between GPS reference clock and the receiver clock,  $dt^{sat}$  is the difference between GPS reference clock and the GPS satellite clock,  $rel$  is the relativistic effect on the signal,  $M_{P_c}$  is the multipath of the combination, and  $\varepsilon_{P_c}$  is the thermal noise and other unmodeled effects.

Nevertheless, with antispoofing activated, the measurements of  $P_1$  and  $P_2$  are much noisier than the ones of  $C/A$  (coarse acquisition code). For this reason, this observable has been chosen instead of  $P_1$ , thus redefining  $P_C$ :

$$P_C = \frac{f_1^2 C/A - f_2^2 P_2}{f_1^2 - f_2^2} = \rho + c(dt_{rec} - dt^{sat}) + rel + M_{P_C} + TGD + \varepsilon_{P_C} \quad (2)$$

where  $TGD$  is the instrumental delay difference between  $C/A$  and  $P_1$ . Note that, despite instrumental delays for the ionospheric-free combination being defined as zero, this is only true when the combination is obtained using  $P_1$  and  $P_2$ . However, when  $P_C$  is computed using  $C/A$  instead of  $P_1$ ,  $TGD$  must be added into the equation.

Therefore, Equation (2) is the main observable used for the LEO satellite real time positioning. But, in order to isolate the multipath,  $M_{P_C}$ , in the *a priori* process,  $L_C$  must be used:

$$L_C = \frac{f_1^2 L_1 - f_2^2 L_2}{f_1^2 - f_2^2} = \rho + c(dt_{rec} - dt^{sat}) + rel + BIAS_{L_C} + m_{L_C} + \varepsilon_{L_C} \quad (3)$$

where  $BIAS_{L_C}$  is the unknown phase ambiguity and  $m_{L_C}$  is the phase multipath. The wind-up term is neglected and inserted as unmodeled noise into  $\varepsilon_{L_C}$ .

Using Equations (2) and (3), the following equation is used to isolate the multipath in the *a priori* process:

$$P_C - L_C = M_{P_C} + B_C + \varepsilon \quad (4)$$

where  $m_{L_C}$  has been neglected and  $B_C$  is an unknown constant value for each arc (it is the contribution of  $BIAS_{L_C}$ , from Equation (3) and  $TGD$  from Equation (2)). The value of  $B_C$  must be estimated for each cycle-slip of any  $L_1$  or  $L_2$ .

Equation (4) provides two unknowns per pseudo-observation that need to be estimated:  $M_{P_C}$  and  $B_C$ .

The second term is kept constant along an arc and the first one is different for each observation, but similar for close rays due to the geometric nature of multipath. This similarity of the multipath for close rays can be used to group multipath unknowns in the *a priori* postprocessing and estimate a map depending on the azimuth and elevation between the LEO and GPS satellites (always in a LEO body-fixed reference frame). This map is computed with a neural network (a 2D Self-Organizing Map), leading to a cell distribution adapted to multipath variations (irregular grid), with a higher center density where greater variations are detected.

The onboard real time processing uses this *a priori* multipath map estimation and applies the proper corrections, i.e., the values of the cells, to each observable.

### A PRIORI MULTIPATH MAP ESTIMATION

The computation of the *a priori* multipath map is done in postprocessing and on the ground. The period of time used for this estimation should allow for covering most of the possible ray directions that the LEO antenna can receive. Five days of data have been proven to be a good choice. In this context, the process is divided into several steps:

- *Preprocessing*: A few stages are done in order to prepare the data: cycle-slip detection, *TGD* estimation (to correct this term of Equation (2) in the real time processing), and the optimal reference frame determination (to obtain the LEO attitude and compute the azimuth and elevation of each GPS satellite with respect to the LEO body-fixed reference frame).
- *$B_C$  estimation*: Merging all the observations given by Equation (4), a single matrix is created to estimate all the unknowns (bias and multipath unknowns grouped in cells of  $5 \times 5$  degrees). The inversion of this matrix provides an estimation of  $B_C$  for all arcs.
- *Regular grid map*: The  $B_C$  estimated values are then used to recalculate the multipath of each observation, forming cells of  $1 \times 1$  degrees (using Equation (4)).
- *Multipath variation estimation*: From the  $1 \times 1$  map, a value is assigned to each cell proportional to the standard deviation of the multipath values of the nearest cells.
- *Monte Carlo algorithm*: This algorithm distributes thousands of directions across the sky, assigning more directions where more multipath variation is estimated. This will be the training set for the neural network.
- *Self-Organizing Map*: The directions generated are inserted as inputs into this step and the cell centers of the final SOMM are generated

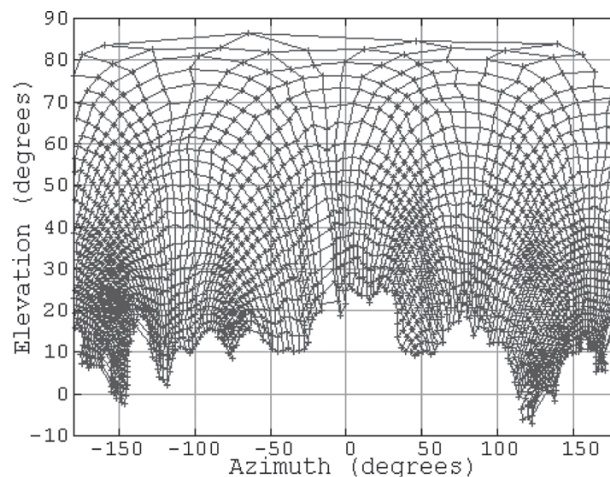


Fig. 2—Center distribution for a Self-Organized Multipath Map (SOMM) computed for SAC-C for days 150 to 154 for 2002. Lines link consecutive indices.

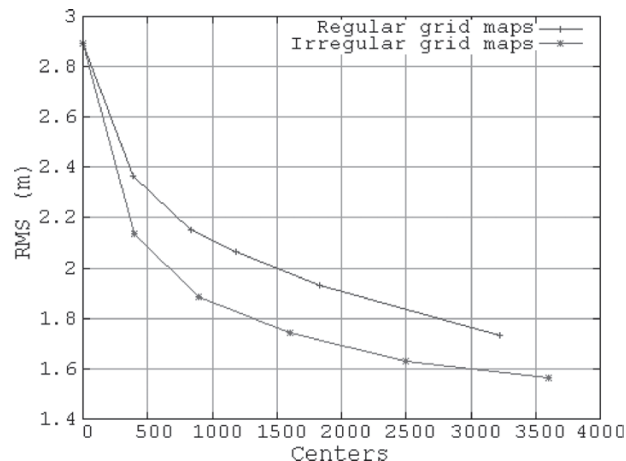


Fig. 3—SAC-C navigation RMS error for day 155 of 2002 using days 150 to 154 to estimate the *a priori* multipath map. Red and blue lines represent regular and irregular maps respectively.

simultaneously to its indexation (with two index values) by means of a self-organizing map [9]. Centers are ordered in such a way that two close cells in the sky have similar indices. This is used to avoid unaffordable searches in real time LEO scenarios (see the *Real Time Multipath Mitigation* section). In Figure 2 the distribution of these cells is shown for a five-day test for a SAC-C satellite. This map has been found to be repeatable for different selections of days.

The advantage of this irregular map in front of a regular one can be seen in Figure 3 for SAC-C satellite, with a reduction of 50% of the centers (i.e., parameters) to get a similar navigation performance. The topological ordering of the map avoids intensive searches through all the centers for each observation.

Afterwards, the SOMM can be transmitted to the LEO satellite (along with the *TGD* information) and the real time process can begin. The images of a  $1 \times 1$  regular grid map and a SOMM are plotted in Figure 4 in order to see the differences between both maps.

## REAL TIME MULTIPATH MITIGATION

The real time process is split into these steps:

- *Preprocessing*: Similar to the *a priori* process, a few stages are done to prepare the data: cycle-slip detection, *TGD* correction, and the optimal reference frame determination.
- *Cell selection*: The closest cell to the direction of each observation is searched by looking at a radius of 2 indices around the previous observation of the same arc (if a cycle-slip was detected a search through all cell centers is performed).
- *Multipath correction*: The proper multipath correction of the selected cell is applied directly to the observable. Another possible approach would be to use a low CPU burden neural algorithm, which has been tested in [10], to allow a real time updating of the cell values.
- *LEO Positioning*: Positioning is performed by means of standard least mean squares and with smoothed and unsmoothed  $P_C$  to compare the results. In order to discard bad measurements, when there are six or more satellites available and the fitting RMS is too high, all the combinations with 1 less satellite are computed and the one with lower RMS is chosen as the final position (as seen in [7] and [11], BlackJack GPS receivers have been reported to have anomalous measurements).

## CPU AND MEMORY COST

The method has been developed to be used in LEO satellites, so it is very important that the real time process can run under low CPU and memory environments. On the other hand, the *a priori* process (to be done on ground facilities) is not a time critical process and can be done in 15 minutes in a Pentium IV desktop computer.

The real time process can be done onboard and the only difference from an unmitigated multipath positioning would be the steps of *Cell selection* and *Multipath correction*. Both steps have low complexity: the *Multipath correction* is simply an addition of a number, and the *Cell selection* is a search over the cells closer to the previously selected cell (thanks to the topology obtained with the Self-Organizing Map, which is an advantage in front of a classic irregular map without topological order-

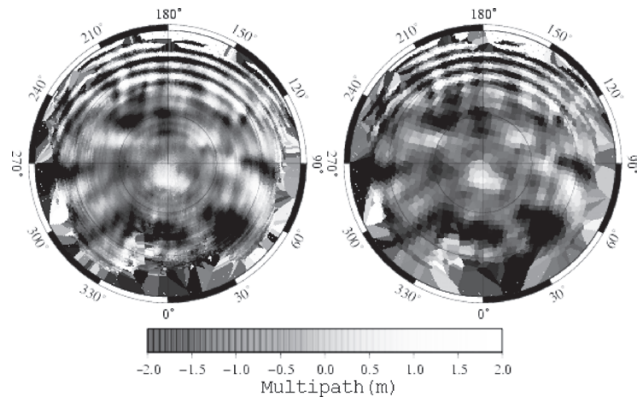


Fig. 4—On left, regular grid map with 26347 centers, on the right, SOMM with 2484 centers. Map for SAC-C for days 150 to 154 for 2002.

ing). As mentioned above, when no cycle-slip is detected, the searching radius is 2 cells (so a total of 25 cells per epoch and satellite are explored), but when a cycle-slip is found, all the map is scanned (for numeric calculations, 2500 centers will be assumed, as this is the grid used in the *Data and Results* section). With the cycle-slip detection algorithm implemented, it is seen that, in mean, 150 cells are explored for each observation, and 7 satellites are in view per epoch, which leads to about 1000 cells explored per epoch.

Each scanned cell is based on the projection of the LoS vector (line of sight) into the cell vector (3D unitary vectors). The cell with major projection of all the scanned cells is the selected cell. Each projection comprises a three dimensional scalar product, which needs three multiplications, two additions and a comparison (against the previous maximum value of the projection). Taking into account that there are, on average, 1000 cells explored per epoch, the requirements of the process are 3000 multiplications, 2000 additions and 1000 comparisons per epoch (on average), which is a low CPU cost for a satellite processor.

The memory requirement is just the storage of the values of the multipath map (13 bits giving 8192 numbers to quantize multipath values, from +20 to -20 in steps of 0.5 cm) and the position of the cells (11 bits for azimuth, from 0 to 360 in steps of 0.25 deg, and 9 bits for elevation, from -10 to +90 in steps of 0.25 deg) which leads to 33 bits per cell \* 2500 cells = 82.5 Kbits  $\approx$  10 KBytes, which is also a negligible contribution to the satellite memory requirements.

## DATA AND RESULTS

GPS observations in RINEX format at a sampling rate of 0.1 Hz from two different LEO satellites have been used: SAC-C and CHAMP (both

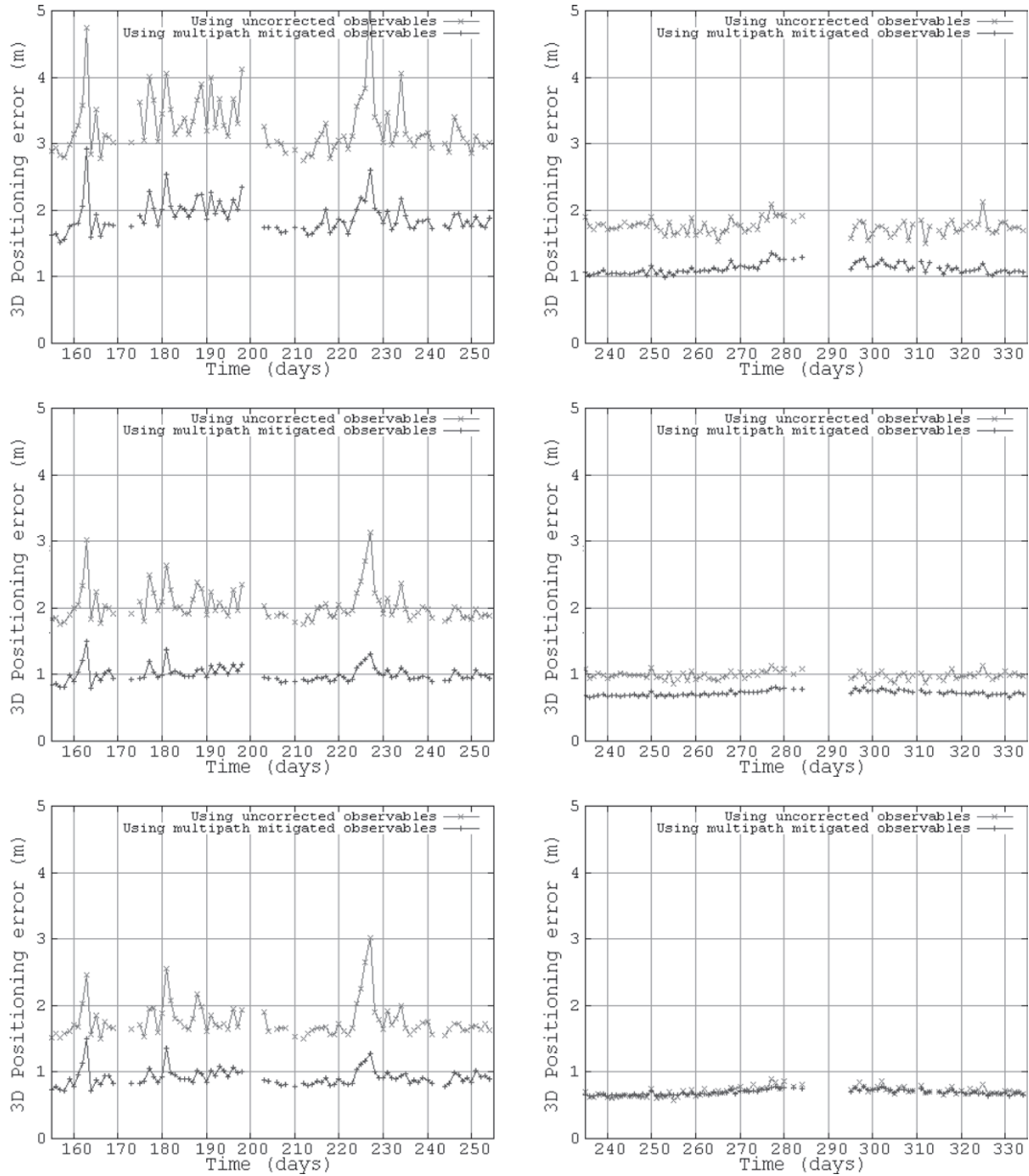


Fig. 5—Daily 3D Positioning error RMS for periods of 100 days in SAC-C (left column, from day 155 to 255) and CHAMP (right column, from day 235 to 335) of 2002. Each point provides the RMS for all the epochs of a single day. First, second, and third rows correspond to unsmoothed, 10 samples smoothed, and 50 samples smoothed observables, respectively.

equipped with dual-frequency BlackJack GPS receivers). The POD antennae of both satellites are zenith oriented. To assess the method, the obtained positions have been compared with the postprocessed precise orbit determination from JPL (available at: <ftp://sayatnova.jpl.nasa.gov>), which have an accuracy of a few centimeters.

The strategy has also been tested using precise IGS clocks and orbits instead of the broadcast ones. Clearly, this is an unrealistic situation, but is done because in this way it is possible to assess the impact of this mitigation in the final navigation solution avoiding the broadcast orbits and clock errors. To be able to make use of this method in a

real time environment, clocks of GPS satellites should be estimated or provided (also using predicted orbits, which have errors slightly higher than the precise ones, but on the order of a few centimeters, so it would not have a large impact on the solution).

The 3D positioning error RMS shown in all results corresponds to the RMS of the 95% of the observations with less error (i.e., the 5% of the total epochs with higher error are discarded, and the remaining ones are used in the RMS computation). This has been done, on one hand, to discard epochs with bad line-of-sight geometries and, on the other hand, to filter out bad measurements,

which can affect the positioning with errors up to tens of meters.

Different smoothing periods have been used with similar results, gaining about 50% improvement in smoothed and unsmoothed observables. The smoothing of the pseudorange using carrier phase observables is a standard procedure and more details can be seen in [12].

In Figure 5, the RMS error position is shown for a full 100 day period for non-smoothed, 10 samples with smoothing, and 50 samples with smoothing for SAC-C and CHAMP satellites.

This multipath mitigation technique significantly improves the navigation solution with the exception of the 50 samples with smoothing in CHAMP. This is a satellite with a very low multipath environment, and, as shown in Figure 6, the larger values of multipath are only reached in the latest part of the arc. In fact, this effect is not due to reflection of signal in the spacecraft structure, but due to cross-talk between the POD and occultation antenna of the receiver (as noted in [7]). This effect has a geometric dependence, so is absorbed into the multipath map. As a consequence of these errors in pseudorange on the later part of the arcs, the bias between  $L_C$  and  $P_C$  (see Equation (4)) can be well estimated from the beginning of the arc with enough smoothing samples. Consequently, for this satellite, the more smoothing samples used, the less the observable is sensitive to geometric dependent errors, and therefore the correction presents a more marginal effect.

In Table 1 the averages of the 100 processed days are shown for both satellites (a value of 1 in smoothing means, in fact, unsmoothed observables).

## CONCLUSIONS AND DISCUSSION

In this work it has been demonstrated that the application of a hybrid offline and real-time multipath mitigation technique based on an artificial neural network significantly improves the navigation solution of LEO satellites with dual frequency receivers. Improvements in 3D positioning accuracy of 40%–50% for SAC-C (obtaining errors of about 90 cm) and of 25%–35% for CHAMP

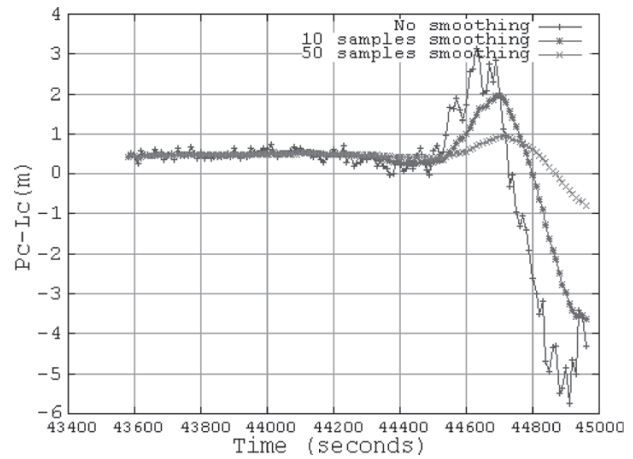


Fig. 6—Unmitigated multipath for a single arc with unknown bias for CHAMP satellite (day 235 of 2002). The effect of applying smoothing with different samples is shown.

(obtaining errors of about 70 cm) have been obtained in the tested periods of 100 days. The technique has low CPU and memory requirements, so it is suitable to be used in low resource environments, such as spacecraft applications.

Moreover, it should be taken into account that the results are heavily dependent on the *a priori* multipath map, so in a real environment, this estimation should be done frequently with special care and testing of its performance before sending it to the LEO satellite. As said, the present work has been done using precise orbits and clocks. Broadcast orbits and clocks have a typical error budget in signal-in-space range errors (SISRE) of about 1–1.5 m [13]. In this case, these errors would be the dominant error source, but applying multipath mitigation would nonetheless enhance the navigation solution. Another option could be the use of predicted ephemerides, which have better performance. This would need an upload of this product with a periodicity of about 6 hours. The mismodeled error mainly due to orbits would decrease, thus increasing the impact of multipath mitigation. Another option would be the use of JPL real-time products, which have a SISRE of about 0.1 m [14]. This would lead to similar results to the ones shown in the paper, but would need a

Table 1—Average of the Positioning Improvement in the Selected Periods for both SAC-C and CHAMP Satellites

Smoothing samples (at 0.1Hz)	3D RMS (m)		Position improvement
	no mitigation	mitigation	
SAC-C 1	3.25	1.89	42%
SAC-C 10	2.03	1.00	51%
SAC-C 50	1.76	0.92	48%
CHAMP 1	1.75	1.12	36%
CHAMP 10	0.99	0.72	27%
CHAMP 50	0.71	0.69	2%

permanent communication link to the satellite, which is still an open problem.

Multipath mitigation is not only useful in the presented context, but it could also provide enhancements in the following points:

- Using carrier phase measurements in the navigation filter. This would increase the computing needs of the filter, but could be feasible depending on the processor of the satellite. As the present method only mitigates pseudorange multipath, it would only have a marginal impact on carrier phase positioning. The advantage this could bring is allowing a faster convergence time after a cycle slip, as pseudorange measurements would have less noise (this would be beneficial for a LEO, which has short arcs on the order of 90–100 minutes).
- Single frequency receivers. The main problem in single frequency receivers would be to obtain the multipath map. The present method makes use of the carrier phase measurements of both frequencies in order to isolate the multipath. Therefore, the offline part of the method would have to change radically. An option to do this would be to use the GRAPHIC combination [15], which would create an ionospheric-free pseudo-observable with multipath and an unknown ambiguity. This combination could be used to simultaneously (onground) estimate LEO positions and clocks, ambiguities, and multipath values. The multipath values obtained would be affected by errors in the GPS orbits and clocks, and the estimation process would be weaker than the one presented in this paper, but could allow for the creation of multipath maps for single frequency receivers.

## ACKNOWLEDGMENTS

The first author would like to thank to the ION GNSS organization for their Student Sponsorship to present the initial version of the paper at ION GNSS 2006.

Part of the work presented in this paper has been done in the frame of the “Neural Networks for Radionavigation” project funded by ESA (under Grant No. ITT4584). The authors would like to thank the project team for their support. In addition, the authors wish to thank the support from the “Departament d’Universitats, Recerca i Societat de la Informació de la Generalitat de Catalunya” and from the European Social Fund, with the additional support of the Spanish projects IBERWARTK and WARTKATNET (references ESP2004-05682-C02-01 and ESP2007-62676, respectively).

Finally, the second author wants to express his debt to his colleague Enric Monte, who introduced him to the neural networks world 17 years ago.

## REFERENCES

1. Montenbruck, O., van Helleputte, T., Kroes, R. and Gill, E., *Reduced Dynamic Orbit Determination using GPS Code and Carrier Measurements*, Aerospace Science and Technology, Vol. 9, No. 3, 2005, pp. 261–271.
2. Kapilal, V., Sparks, A. G., Buffington, J. M. and Qiguo, Yan, *Spacecraft Formation Flying: Dynamics and Control*, Proceedings American Control Conference, Vol. 6, 1999, pp. 4137–4141.
3. Philip, N. K., Krishna Kumar, E. and Ananthasayanan, M. R., *Sliding Observer for a Robust Relative Positioning and Attitude Estimation During the Final Phase of an Autonomous Docking Mission*, Proceedings 49<sup>th</sup> International Astronautical Congress, Melbourne, Australia, 1998.
4. Davies, K., *Ionospheric Radio*, Institution of Electrical Engineers, 1990.
5. Parkinson, B. W. and Spilker, J. J., *Global Positioning System: Theory and Applications*, 1996, pp. 560–566.
6. Reichert, A. K. and Axelrad, P., *Carrier-phase Multipath Corrections for GPS-based Satellite Attitude Determination*, NAVIGATION, Journal of The Institute of Navigation, Vol. 48, No. 2, 2001, pp. 77–88.
7. Montenbruck, O. and Kroes, R., *In-flight Performance Analysis of the CHAMP BlackJack GPS Receiver*, GPS Solutions, Vol. 7, No. 2, 2003, pp. 74–86.
8. Haines, B., Bar-Sever, Y., Bertiger, W., Desai, S. and Willis, P., *One-centimeter Orbit Determination for Jason-1: New GPS-Based Strategies*, Marine Geodesy, Vol. 27, 2004, pp. 299–318.
9. Kohonen, T., *The self-organizing map*, Proceedings IEEE, 78, 1990, pp. 1464–1480.
10. Hernandez-Pajares, M., Juan, J. M. and Sanz, J., *GPS Code Multipath Detection and Mitigation in a LEO Scenario using Neural Networks*, ESA WPP, ISSN 1022-6656, Vol. 173, 2000, pp. 594–622.
11. Williams, J., Lightsey, E. G., Yoon, S. and Schutz, R. E., *Testing of the ICESat BlackJack GPS Receiver Engineering Model*, Proceedings of the 15th International Technical Meeting of the Satellite Division of The Institute of Navigation ION GPS 2002, Portland, USA, 2002, pp. 703–714.
12. *Minimum Operational Performance Standards for Global Positioning System/Wide Area Augmentation System Airborne Equipment*, RTCA, DO-229C, Issued November 2001, p. 46.
13. Warren, D. L. and Raquet, J. F., *Broadcast vs Precise GPS Ephemerides: A Historical Perspective*, GPS Solutions, Vol. 7, No. 3, 2003, pp. 151–156.
14. Bar-Sever, Y., Muellerschoen, R., Reichert, A., Vozoff, M. and Young, L., *The Development and Demonstration of NASA’s Global Differential System*, Proceedings of ESTEC 2002, Pasadena, USA, 2002.
15. Yunck T. P., *Coping with the Atmosphere and Ionosphere in Precise Satellite and Ground Positioning, Environmental Effects on Spacecraft Trajectories and Positioning*, AGU Monograph, 1993.